Mode expansion description of stadium-cavity laser dynamics

Susumu Shinohara,[1] Satoshi Sunada,[1,2] Takahisa Harayama,[1] and Kensuke S. Ikeda[2]
[1]*Department of Nonlinear Science, ATR Wave Engineering Laboratories, 2-2-2 Hikaridai, Seika-cho, Soraku-gun, Kyoto, 619-0288, Japan*
[2]*Department of Physical Sciences, Ritsumeikan University, 1-1-1 Noji-higashi, Kusatsu, Shiga, 525-8577, Japan*
(Received 29 October 2004; published 11 March 2005)

The lasing dynamics of a stadium-cavity laser is studied by using a mode expansion model which is a reduction of the Schrödinger-Bloch model. We study the properties of stationary lasing states when two cavity modes are selectively excited, while examining the validity of the mode expansion model by comparing its results with those of the Schrödinger-Bloch model. Some analytical results are obtained for single-mode and two-mode stationary lasing states for the mode expansion model.

DOI: 10.1103/PhysRevE.71.036203 PACS number(s): 05.45.−a, 42.55.Sa, 42.65.Sf

I. INTRODUCTION

In studying lasing in two-dimensional (2D) lasers, it is essential to elucidate the properties of cavity modes, especially the ones with low loss [1–3]. Moreover, in order to properly describe stationary lasing states supported by external pumping, it is necessary to take into account the nonlinear interaction among the cavity modes. So far, nonlinear dynamical treatment of 2D lasers has been carried out with the Schrödinger-Bloch (SB) model [4,5]. The SB model, derived from the Maxwell equations and the optical-Bloch equations, describes nonlinear interaction between the light field and a two-level gain medium. Some of the present authors have performed numerical simulations on the SB model with a stadium cavity, and demonstrated that stationary lasing states can be well explained by the properties of the cavity modes. For example, the lasing pattern of a single-mode stationary state was shown to be quite similar to that of a cavity-mode eigenfunction [4], and some intriguing multimode interactions were revealed, one of which being the frequency locking of two different-parity modes [5]. We note that recently semiconductor laser diodes with a stadium cavity were actually fabricated, and stable lasing has been experimentally confirmed [6]. Moreover, asymmetric far-field patterns experimentally observed in quasistadium-cavity lasers have been successfully explained by the frequency-locking phenomenon [5,6].

According to the results of the SB model simulation, the dynamics seem to be well described in terms of the mode concept. Thus one may expect that the dynamics of the original partial differential equation model can be essentially described by an ordinary differential equation model which is obtained, for instance, by expanding the electromagnetic field by mode basis functions. Such a reduction of the model is desirable for a more comprehensive analysis based upon the nonlinear dynamics theory.

In this paper, focusing on a stadium cavity case, we consider a reduction of the SB model to a mode expansion model, which we shall call the mode-expanded Schrödinger-Bloch (MSB) model. We employ closed-cavity modes as the mode basis, phenomenologically incorporating the effect of energy leakage at the cavity boundary. Such treatment is common in the studies of 1D lasers [7]. However, it is not so clear to what extent the phenomenological treatment works when the light emission becomes two dimensional. Thus, in order to confirm the validity of the modal description, we compare the results of the MSB model with those of the SB model. It is demonstrated that, concerning single-mode and two-mode lasing, the MSB model reproduces characteristic features of the SB model. Moreover, the introduction of the MSB model allows us to obtain analytical results on single-mode and two-mode stationary lasing states.

This paper is organized as follows. In Sec. II, we review the results of the SB model, mainly focusing on single-mode and two-mode lasing. In Sec. III, we derive the MSB model from the SB model, and study its dynamics theoretically and numerically. Section IV is a summary.

II. SCHRÖDINGER-BLOCH MODEL

In this section, we review the dynamical simulation of the SB model. First, let us introduce the SB model. When the cavity is wide in the *xy* directions and thin in the *z* direction compared to the light wavelength, the SB model is given as follows [4,5]:

$$\frac{\partial \tilde{E}}{\partial t} = \frac{i}{2}\left(\nabla_{xy}^2 + \frac{n^2}{n_{in}^2}\right)\tilde{E} - \alpha\tilde{E} + \mu\tilde{\rho}, \tag{1}$$

$$\frac{\partial \tilde{\rho}}{\partial t} = -(\tilde{\gamma}_\perp + i\Delta_0)\tilde{\rho} + \tilde{\kappa}W\tilde{E}, \tag{2}$$

$$\frac{\partial W}{\partial t} = -\tilde{\gamma}_\parallel(W - W_\infty) - 2\tilde{\kappa}(\tilde{E}\tilde{\rho}^* + \tilde{E}^*\tilde{\rho}), \tag{3}$$

where $\tilde{E}(x,y,t)$ and $\tilde{\rho}(x,y,t)$ are the slowly varying envelopes of the TM electric field and of the polarization field, respectively, and $W(x,y,t)$ is the population inversion component. The cavity shape determines the spatial distributions of both the refractive index n and the cavity absorption coefficient α; $n(x,y)$ is n_{in}(const) inside the cavity and n_{out}(const) outside the cavity, while $\alpha(x,y)$ is α_L(const) inside the cavity and zero outside the cavity. Space and time are made dimensionless by the scale transformations

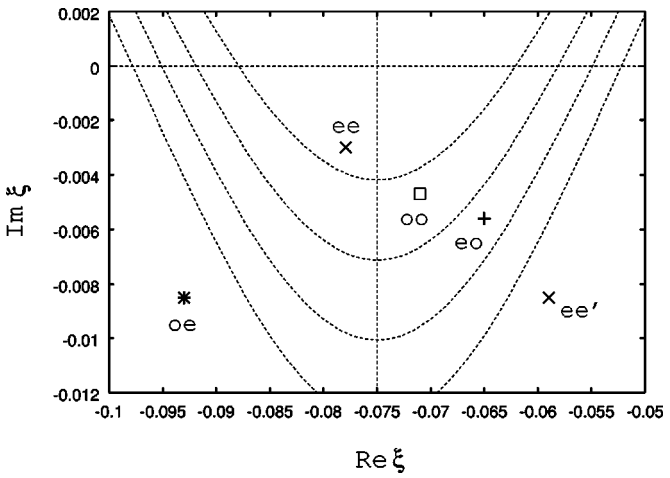

FIG. 1. A distribution of the complex eigenvalues. The dashed curves are the lower boundaries of the positive gain region for $W_\infty = 0.0045$, 0.0048, 0.0051, 0.0054 (from top to bottom).

$(n_{in}\omega_s x/c, n_{in}\omega_s y/c) \to (x,y)$ and $t\omega_s \to t$, respectively, with ω_s being the oscillation frequency of the light field slightly different from the transition frequency ω_0 of the two-level medium. The difference of the two frequencies can be measured by a parameter $\Delta_0 = (\omega_0 - \omega_s)/\omega_s$, which plays the role of the gain center. The other parameters are as follows: $\tilde{\gamma}_\perp$ and $\tilde{\gamma}_\parallel$ are, respectively, the transversal and longitudinal relaxation rates, μ and $\tilde{\kappa}$ represent the coupling strength between the light field and the medium, and W_∞ is the external pumping strength.

For the numerical simulation of the SB model, we employ specific settings: we fix the cavity shape to be a stadium consisting of two half circles of the radius $R = 49/4\sqrt{2}$ and two flat lines of the length $2R$; moreover, we set the values of most of the system's parameters as follows: $n_{in} = 2$, $n_{out} = 1$, $\Delta_0 = -0.075$, $\alpha_L = 4 \times 10^{-2}$, $\gamma_\perp = 4 \times 10^{-2}$, $\gamma_\parallel = 2 \times 10^{-2}$, $\tilde{\kappa} = 0.5$, and $\mu = \pi/4$.

As was demonstrated in Refs. [4,5,8], a key to understanding the SB model's dynamics is the identification of the cavity modes. The cavity modes $u_k(x,y)$ ($k = 1, 2, \ldots$) are the solutions of the Helmholtz equation

$$-\frac{1}{2}\left(\nabla_{xy}^2 + \frac{n^2}{n_{in}^2}\right) u_k(x,y) = \xi_k u_k(x,y), \tag{4}$$

where the eigenvalue ξ_k becomes complex because the cavity is an open system. The complex eigenvalues (resonances) ξ_k and eigenfunctions $u_k(x,y)$ can be calculated by the extended boundary element method [4,9].

Figure 1 shows a distribution of the complex eigenvalues around $\mathrm{Re}(\Delta) = \Delta_0$. The eigenvalues are also listed in Table I. Because the stadium cavity has reflection symmetry with respect to both the x and y axes, an eigenfunction u_k satisfies $u_k(-x,y) = a u_k(x,y)$ and $u_k(x,-y) = b u_k(x,y)$ with $a, b = \pm 1$. Thus the eigenmodes are classified into four parity classes labeled by *even-even* ($a = b = +1$), *even-odd* ($a = 1, b = -1$), *odd-even* ($a = -1, b = +1$), and *odd-odd* ($a = b = -1$).

We chose the value of Δ_0 so that the two adjacent modes labeled by *ee* and *oo* can preferentially attain the gain. Note

TABLE I. The complex eigenvalues of the open-cavity system.

mode	$\mathrm{Re}(\xi_k)$	$\mathrm{Im}(\xi_k)$
ee	−0.0780	−0.0035
oo	−0.0709	−0.0049
eo	−0.0650	−0.0060
ee′	−0.0591	−0.0090
oe	−0.0934	−0.0087

that the positive gain region of the ξ plane is defined as follows [4]:

$$\frac{\mu\tilde{\kappa}\tilde{\gamma}_\perp W_\infty}{\tilde{\gamma}_\perp^2 + [\mathrm{Re}(\xi_k) - \Delta_0]^2} > -\mathrm{Im}(\xi_k) + \alpha_L. \tag{5}$$

Such regions are indicated in Fig. 1 for several W_∞ values.

For various W_∞ values, we numerically integrate Eqs. (1)–(3) for long times (typically $t \approx 10^5$) to obtain stationary states. Figure 2 shows the pumping strength dependence of the total light intensity inside the cavity for the stationary state. The lasing threshold is evaluated to be $W_\infty \approx 0.0045$, and a slight change of the slope at $W_\infty \approx 0.0078$ is due to a frequency-locking phenomenon explained below. Just above the lasing threshold, we obtain a single-mode lasing stationary state where only the mode *ee* lases. This can be confirmed by the power spectrum of the time series of the electric field at a certain point in the cavity as shown in Fig. 3(a).

For $0.0050 \lesssim W_\infty \lesssim 0.0078$, we have a two-mode lasing state where most of the energy is retained by the two modes *ee* and *oo*, and these modes oscillate with different frequencies. A typical power spectrum for the two-mode lasing state is shown in Fig. 3(b). The frequency difference becomes smaller when we increase the W_∞ value, and eventually at $W_\infty \approx 0.0078$, the two frequencies merge, or frequency locking occurs. As a consequence of this frequency locking of the two different-parity modes, the lasing pattern becomes asymmetric [5]. We plot the W_∞ dependence of the frequencies in

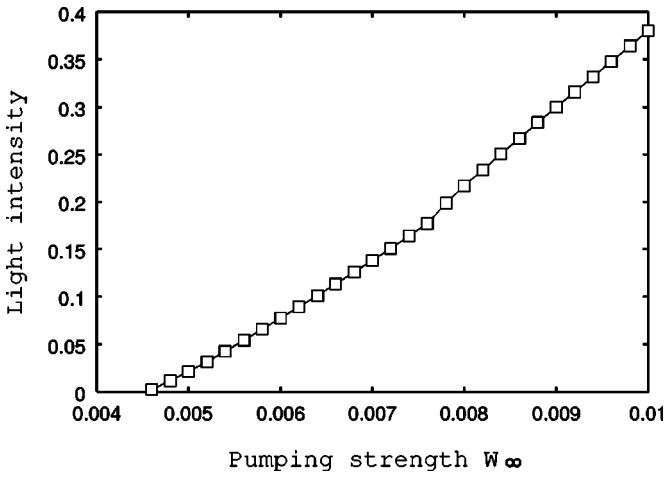

FIG. 2. Light intensity inside the cavity vs the pumping strength W_∞ for the SB model.

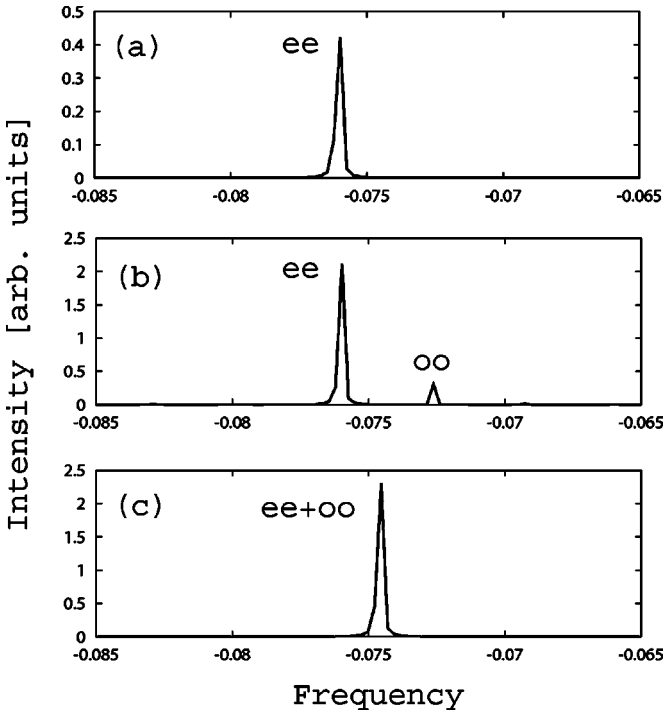

FIG. 3. Power spectra of $\tilde{E}(t)$ for stationary lasing states of the SB model; (a) $W_\infty=0.0048$, (b) $W_\infty=0.0060$, and (c) $W_\infty=0.0080$.

Fig. 4. An intriguing feature of the frequency-locking phenomenon is that most of all the energy is occupied by the frequency-locked state labeled by *ee+oo*, even when many other modes are in the positive gain region. This can be confirmed by the power spectrum shown in Fig. 3(c). We numerically checked that the dominancy of the frequency-locked state continues beyond $W_\infty=0.02$.

III. MODE EXPANSION DESCRIPTION

A. Mode-expanded Schrödinger-Bloch model

Now, we construct a mode expansion version of the SB model. The open-cavity modes are characterized by complex eigenvalues, and are, in general, not guaranteed to form a

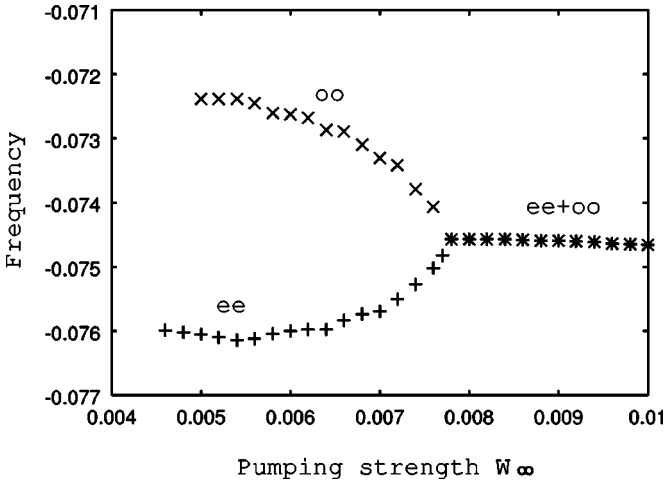

FIG. 4. The dependence of mode frequencies on the pumping strength W_∞ for the SB model.

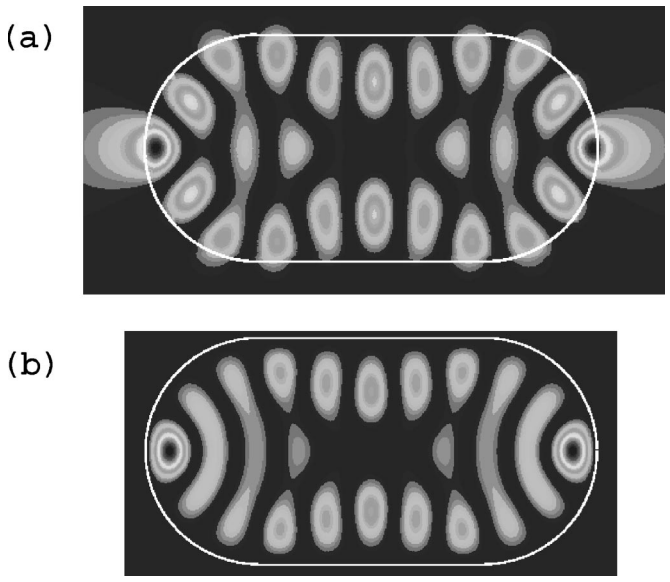

FIG. 5. (a) The eigenfunction of the open-cavity mode *ee*. (b) The eigenfunction of the closed-cavity mode corresponding to the open-cavity mode *ee*.

complete basis [10]. Therefore we instead use the closed-cavity modes for the expansion of the variables, phenomenologically taking into account the effects of energy leakage at the cavity boundary. The closed-cavity modes are nothing but eigenmodes of Eq. (4) with the infinite-wall boundary condition. In the wavelength regime of our interest, we were able to make a correspondence between the open-cavity modes and the closed-cavity modes by comparing the nodal patterns of eigenfunctions. An example of the correspondence is presented in Fig. 5.

Let us denote the normalized closed-cavity modes by $v_k(x,y)$. Expanding $\tilde{E}$ and $\tilde{\rho}$ as $\tilde{E}=\Sigma_k E_k(t)v_k(x,y)$ and $\tilde{\rho}=\Sigma_k \rho_k(t)v_k(x,y)$, respectively, we obtain the MSB model as follows:

$$\frac{dE_k}{dt} = -(\alpha_L + \alpha_k + i\Delta_k)E_k + \mu\rho_k, \tag{6}$$

$$\frac{d\rho_k}{dt} = -(\tilde{\gamma}_\perp + i\Delta_0)\rho_k + \tilde{\kappa}W_\infty E_k + \tilde{\kappa}\sum_l w_{kl}E_l, \tag{7}$$

$$\frac{dw_{kl}}{dt} = -\tilde{\gamma}_\parallel w_{kl} - 2\tilde{\kappa}\sum_m\sum_n J_{klmn}(E_m\rho_n^* + E_m^*\rho_n), \tag{8}$$

with

$$w_{kl}(t) = \iint_{\mathcal{D}} dxdy\,[W(x,y,t) - W_\infty]v_k v_l(x,y), \tag{9}$$

$$J_{klmn} = \iint_{\mathcal{D}} dxdy\, v_k v_l v_m v_n(x,y), \tag{10}$$

where $\mathcal{D}$ is the area inside the cavity. In order to incorporate the effect of the energy leakage, we introduced mode-

dependent decay rates α_k in Eq. (6). Since the imaginary part of an eigenvalue characterizes the decay rate of the mode, we put $\alpha_k=|\mathrm{Im}(\xi_k)|$. Moreover, we substitute the mode's eigenfrequency Δ_k with the real part of the complex eigenvalue, i.e., $\Delta_k=\mathrm{Re}(\xi_k)$.

Although the mode expansion is formulated with an infinite number of modes, we shall take into account only the modes located near the gain center. Note that if the modes outside the positive gain region are never to be excited, i.e., $E_k(t)\equiv 0$, the above system is closed within the modes inside the positive gain region.

In the MSB model, the effect of the cavity shape appears through the mode-coupling coefficients J_{klmn} and the parameters α_k and Δ_k. Compared to 1D-cavity cases, a prominent difference of 2D-cavity cases is the absence of "strong" mode-interaction rules, although we might still have "weak" rules when the cavity has some symmetry. For instance, in the case of a stadium cavity, its symmetry leads to some constraints on the mode interaction. That is, the mode-coupling coefficient J_{klmn} is nonzero if and only if either of the following is satisfied: (i) the parities of the four modes k, l, m, n are all different; (ii) the parities of the four modes k, l, m, n are all the same; or (iii) the four modes k, l, m, n consist of two same-parity pairs. The values of nonzero J_{klmn} are determined by numerically calculating Eq. (10).

B. Single-mode and two-mode lasing

Here, we study the dynamics of the MSB model with the same parameters as used for the SB model simulation in Sec. II, and examine the validity of the mode expansion approach, comparing the results of the MSB model with those of the SB model. The reduction of the PDE model to the ODE model enables us to obtain some analytical results for stationary lasing states. In the numerical simulation of the MSB model presented below, we include five modes near the gain center, labeled by *ee*, *oo*, *eo*, *ee′*, and *oe*, to construct the MSB model.

First, we study single-mode lasing. For the MSB model, one can derive the single-mode stationary solution analytically. Assuming that only the sth mode has positive gain, and that the stationary solution has the form $E_s=\overline{E_s}e^{i\phi}$, $\rho_s=\overline{\rho_s}e^{i\phi}$, and $w_{ss}=\mathrm{const}(\overline{E_s},\phi,w_{ss}\in\mathbb{R},\overline{\rho}\in\mathbb{C})$, we obtain

$$I=\overline{E_s^2}=\frac{\tilde{\gamma}_{\parallel}\mu}{4\tilde{\kappa}J_{ssss}\alpha_{tot}}(W_\infty-W_\infty^{(0)}), \tag{11}$$

$$\frac{d}{dt}\phi=-\frac{\alpha_{tot}\Delta_0+\tilde{\gamma}_\perp\Delta_s}{\alpha_{tot}+\tilde{\gamma}_\perp}, \tag{12}$$

where $\alpha_{tot}=\alpha_L+\alpha_s$ is the total loss rate and $W_\infty^{(0)}$ is the lasing threshold given by

$$W_\infty^{(0)}=\frac{\alpha_{tot}\tilde{\gamma}_\perp}{\tilde{\kappa}\mu}\left\{1+\left(\frac{\Delta_0-\Delta_s}{\alpha_{tot}+\tilde{\gamma}_\perp}\right)^2\right\}. \tag{13}$$

Note that the linear dependence of the light intensity on the pumping strength is reproduced by the MSB model.

A quantitative comparison of the two models is given in Table II. Compared to the good agreement of the lasing threshold, the difference of the slope dI/dW_∞ is noticeable. This might be caused by overestimating the value of the coupling coefficient J_{ssss} because of the following reason. In calculating the value of J_{ssss} from Eq. (10), we supposed a stadium with $R=49/4\sqrt{2}$. However, as can be seen from Fig. 5, an eigenfunction of the open cavity is extended compared to that of the closed cavity. Since J_{klmn} scales as R^{-2}, the use of a smaller R value yields a larger J_{klmn} value. Although the extension of the eigenfunction is nonuniform, the average extension rate is roughly estimated as 1.1. This corrects the value of dI/dW_∞ for the MSB model to be 46.2.

TABLE II. Comparison of the SB and MSB models with regard to single-mode lasing.

	Lasing threshold	dI/dW_∞
SB model	0.00455	45.8
MSB model	0.00444	38.2

Next, we consider the cases where the W_∞ value is large enough for multimode lasing. In Fig. 6, the W_∞ dependences of the total light intensity $\Sigma_k E_k^2$ and its mode components E_k^2 are plotted. We can see that the modes *ee* and *oo* constitute the main components for $W_\infty\lesssim 0.01$. For these two modes, we plot the W_∞ dependence of the frequencies in Fig. 7, where we can see that the frequency-locking phenomenon is reproduced. The frequency-locking threshold is estimated to be $W_\infty\approx 0.0064$, which is 18% smaller than the threshold for the SB model. Although there is such a quantitative difference, it is remarkable that, in the frequency-locking regime, almost all the energy is shared by the modes *ee* and *oo*, while the other modes are located deep inside the positive gain region. This is consistent with the SB model's results, providing evidence that the mode-interaction effect of the SB model is properly inherited by the MSB model. However, for much larger W_∞ values ($W_\infty\gtrsim 0.01$), modes other than *ee* and *oo* start to lase, which is qualitatively different from the SB model's results. Since the mode is basically defined for a linear system, the breakup of the mode-based description appears to be unavoidable for too large nonlinearity.

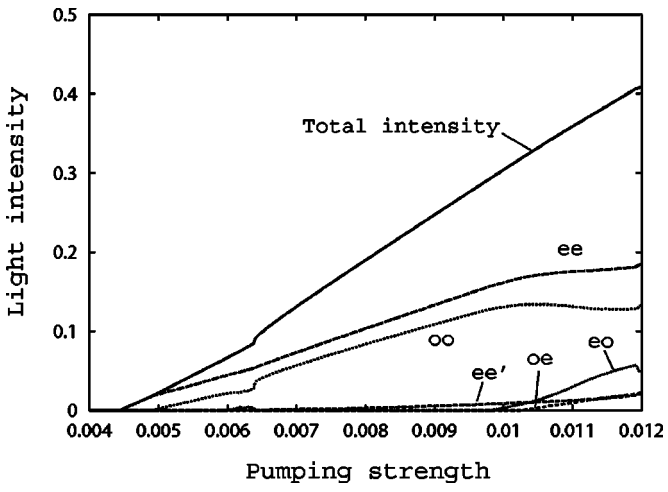

FIG. 6. Light intensities I and $E_k^2(k=1,\ldots,5)$ vs the pumping strength W_∞ for the MSB model.

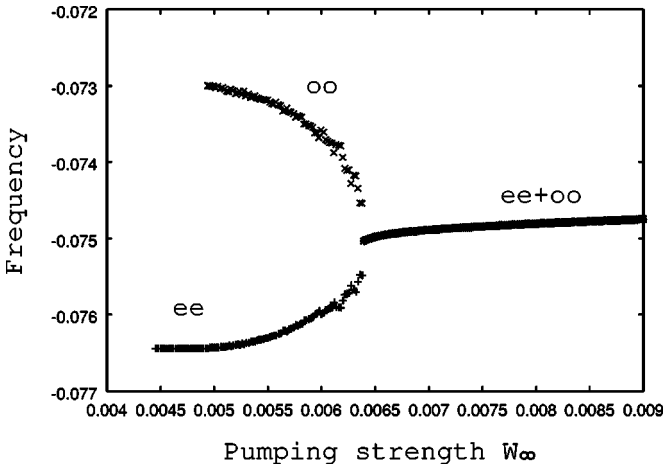

FIG. 7. The dependence of mode frequencies on the pumping strength W_∞ for the MSB model.

Finally, we focus on the frequency-locking phenomenon of the MSB model. In the frequency-locking regime, the dynamics can be approximately described by the two modes *ee* and *oo*. Labeling the modes *ee* and *oo* by $k=1$ and $k=2$, respectively, we assume the frequency-locked stationary solutions as follows: $E_k=\overline{E_k}e^{i\phi_k}$, $\rho_k=\overline{\rho_k}e^{i\phi_k}$, $w_{kl}=\text{const}$ $(\overline{E_k},\phi_k,w_{kl}\in\mathbb{R},\overline{\rho_k}\in\mathbb{C};k,l=1,2)$, where $d\phi_1/dt=d\phi_2/dt=-\nu$. Substituting these into Eqs. (6)–(8), one obtains a set of equations that determines the W_∞ range where the frequency-locked solution exists. Since the equations are too complicated to be analytically solved for a general case, we consider here an idealized case to which we can derive the locking threshold exactly. Namely, we consider a case where the two complex eigenvalues are symmetrically placed with respect to the gain center line, i.e., $\alpha_1=\alpha_2=\overline{\alpha}$ and $d_1=d_2=d$ with $d_k=|\Delta_k-\Delta_0|$. Besides, we assume $J_{1111}=J_{2222}=J$. After this approximation, we can derive the locking threshold as follows:

$$W_\infty^{(1)}=\frac{\alpha_{tot}\tilde{\gamma}_\perp}{\tilde{\kappa}\mu}\left\{1+\frac{\cos\delta}{\sin^2\delta}(\beta\cos\delta+\sqrt{\beta^2-1})\right\}, \quad (14)$$

where $\alpha_{tot}=\alpha_L+\overline{\alpha}$, $\delta=\arctan(\alpha_{tot}/d)$ and $\beta=\overline{J}/J_{1122}+2$. In the case of $\alpha_{tot}\gg d$, this reduces to

$$W_\infty^{(1)}\approx\frac{\alpha_{tot}\tilde{\gamma}_\perp}{\tilde{\kappa}\mu}\left(1+\frac{d}{\alpha_{tot}}\sqrt{\beta^2-1}\right). \quad (15)$$

In Fig. 8, we plot the dependence of $W_\infty^{(1)}$ on the parameters α_{tot} and $\tilde{\gamma}_\perp$, while the other parameters are fixed at the values given in Sec. II, and we put $\overline{\alpha}=(\alpha_1+\alpha_2)/2$. In Fig. 8, theoretical curves given by Eq. (14) are also plotted. For these theoretical curves, we supposed $d=(d_1+d_2)/2\approx 0.003\,55$ and $\beta=\frac{1}{2}(J_{1111}+J_{2222})/J_{1122}+2\approx 4.96$, where the mode coupling coefficients are calculated from Eq. (10) as $J_{1111}=0.004\,72$, $J_{2222}=0.004\,84$, and $J_{1122}=0.001\,61$. It turns out that, in spite of the crude approximation, the theoretical estimate well explains the numerical data. Since the determination of the threshold for the SB model requires an enormous amount of numerical computation, the theoretical estimation is useful for knowing the qualitative nature of the frequency-locking phenomenon.

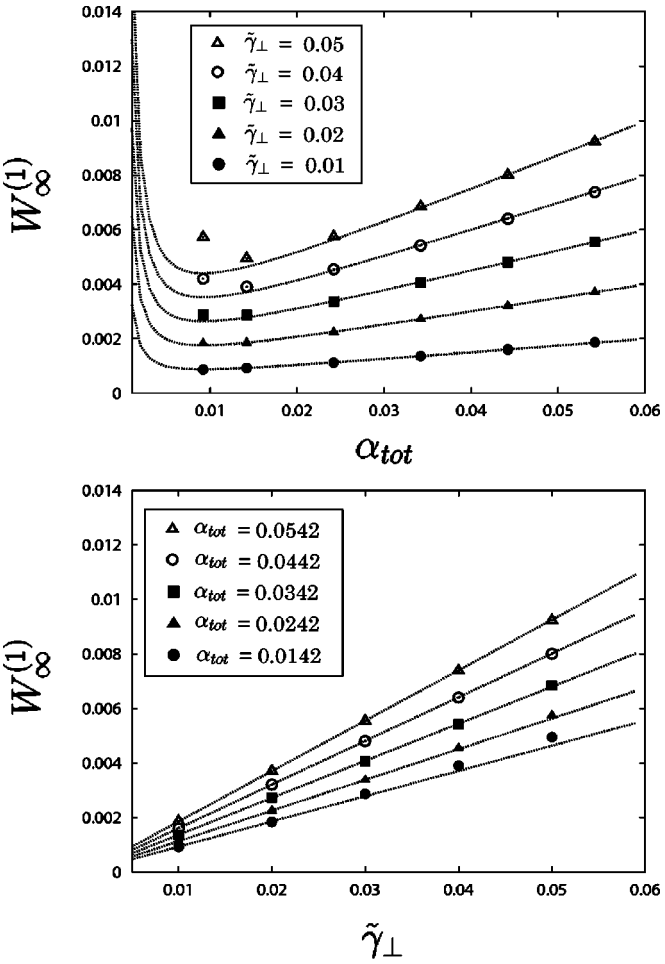

FIG. 8. The parameter dependence of the frequency-locking threshold $W_\infty^{(1)}$ for the MSB model. The dotted curves are theoretical ones given by Eq. (14).

IV. SUMMARY

By constructing a mode expansion version of the SB model, we studied the properties of stationary lasing states when two modes are selectively excited. The validity of the mode expansion description was examined by comparing the results of the MSB model with those of the SB model. It was demonstrated that qualitative features of the SB model simulation could be reproduced by the MSB model, provided that the nonlinearity is not too strong to invalidate the description based on the linear modes. The introduction of the MSB model enabled us to analytically study the stationary states to some extent. In particular, we were able to obtain an analytical expression for the frequency-locking threshold.

ACKNOWLEDGMENT

The work at ATR was supported in part by the National Institute of Information and Communications Technology of Japan.

[1] *Optical Processes in Microcavities*, edited by R. K. Chang and A. J. Campillo (World Scientific, Singapore, 1996).
[2] J. U. Nöckel and A. D. Stone, Nature (London) **385**, 45 (1997).
[3] C. Gmachl, F. Capasso, E. E. Narimanov, J. U. Nöckel, A. D. Stone, J. Faist, D. L. Sivco, and A. Y. Cho, Science **280**, 1556 (1998).
[4] T. Harayama, P. Davis, and K. S. Ikeda, Phys. Rev. Lett. **90**, 063901 (2003).
[5] T. Harayama, T. Fukushima, S. Sunada, and K. S. Ikeda, Phys. Rev. Lett. **91**, 073903 (2003).
[6] T. Fukushima and T. Harayama, IEEE J. Sel. Top. Quantum Electron. **10**, 1039 (2004).
[7] M. Sargent III, M. O. Scully, and W. E. Lamb, Jr., *Laser Physics* (Addison-Wesley, Reading, MA, 1974).
[8] S-Y. Lee, M. S. Kurdoglyan, S. Rim, and C-M Kim, Phys. Rev. A **70**, 023809 (2004).
[9] J. Wiersig, J. Opt. A, Pure Appl. Opt. **5**, 53 (2003).
[10] A. E. Siegman, *Lasers* (University Science Books, Mill Valley, CA, 1986).